

## 77 K operation of AlGaAs/GaAs quantum cascade laser at 9 $\mu\text{m}$

Kamil Kosiel<sup>\*1</sup>, Maciej Bugajski<sup>1</sup>, Anna Szerling<sup>1</sup>, Justyna Kubacka-Traczyk<sup>1</sup>, Piotr Karbownik<sup>1</sup>, Emilia Pruszyńska-Karbownik<sup>1</sup>, Jan Muszalski<sup>1</sup>, Adam Łaszcz<sup>1</sup>, Przemek Romanowski<sup>2</sup>, Michał Wasiak<sup>3</sup>, Włodzimierz Nakwaski<sup>3</sup>, Irina Makarowa<sup>4</sup>, Piotr Perlin<sup>4</sup>

<sup>1</sup>Institute of Electron Technology, Al.Lotników 32/46, 02-668 Warszawa,

<sup>2</sup>Institute of Physics, Polish Academy of Sciences, Al.Lotników 32/46, 02-668 Warszawa

<sup>3</sup>Institute of Physics, Technical University of Łódź, Wólczańska 219, 93-005 Łódź,

<sup>4</sup>TopGaN, Sokołowska 29/37, 01-142 Warszawa

Received February 19, 2009; accepted March 12, 2009; published March 31, 2009

**Abstract**—The cryogenic-temperature (77 K), pulsed mode operation of GaAs-based quantum cascade laser (QCL) is reported. This has been achieved by the use of GaAs/Al<sub>0.45</sub>Ga<sub>0.55</sub>As heterostructure. The laser design followed an “anticrossed-diagonal” scheme of Page *et al.* [1]. The QCL structures were grown by MBE, with Riber Compact 21T reactor. The double trench lasers were fabricated using standard processing technology, i.e., wet etching and Si<sub>3</sub>N<sub>4</sub> for electrical insulation. Double plasmon confinement with Al-free waveguide has been used to minimize absorption losses.

The quantum cascade lasers (QCLs) are unipolar devices based on tunneling and intersubband transitions, in which the electronic states, wavefunctions and lifetimes of relevant states are engineered through the quantum mechanical confinement imposed by a complex multilayer structure. The GaAs-based QCLs have proved to be an effective source of laser radiation in mid-infrared (MIR) as well as far-infrared (FIR) regions.

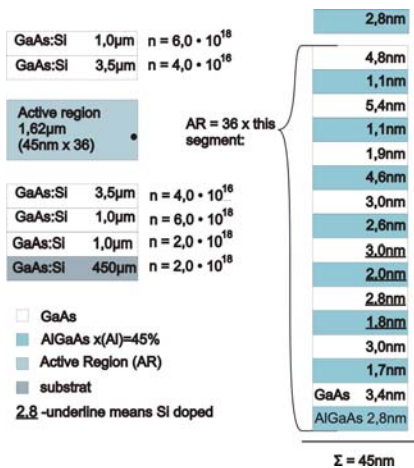


Fig. 1 Layer sequence in the Al<sub>0.45</sub>Ga<sub>0.55</sub>As/GaAs laser structure

The laser structure studied in this paper (Fig.1) was the 36 period sequence of injector+3QW active region, made of Al<sub>0.45</sub>Ga<sub>0.55</sub>As/GaAs-coupled quantum wells.

\* E-mail: kosiel@ite.waw.pl

The active region was based upon the three quantum well design. The injector doping was  $\sim 2.2 \times 10^{12} \text{cm}^{-2}$  per period. Only two barrier-QW pairs in the central part of each injector have been doped. The structure used double-plasmon Al-free waveguide for planar optical confinement.

The electronic band structure of QCL has been calculated by solving Schroedinger equation with position dependent effective mass by finite difference method (FDM) [2] – see Fig.2.

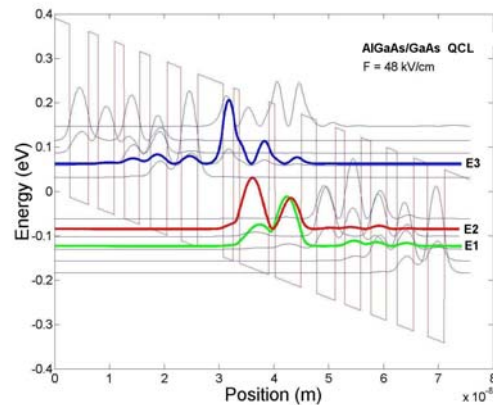


Fig. 2 Conduction band profile and moduli squared wavefunctions in injector/active/injector segment of the laser under the applied field of 48 kV/cm. The wavefunctions have been shifted to the energy positions of the respective levels. The E3, E2 and E1 refer to the upper, lower and ground state of lasing transitions. The thin blue lines are the injector miniband states. The lowest energy state in the injector couples directly to the upper laser level E3. The topmost state is the  $\Gamma$  continuum state. It is located  $\sim 80$  meV above the upper laser level. The calculated energy differences  $E_{32}=147.1$  meV ( $\lambda=8.4$   $\mu\text{m}$ ) and  $E_{21}=38.5$  meV.

The essential features of the considered design are diagonal anti-crossed transitions from state E3 to E2 and depopulation of the laser ground state E2 by resonant optical phonon emission and tunneling into the injector. The calculated lifetime of the excited state and dipole matrix element are  $\tau_3=1.4$  ps, and  $z_{32}=1.71$  nm, respectively. The ground state E2 is depopulated in the

time  $\tau_{2,1} \sim 0.3$  ps [1]. These calculations were done at 48 kV/cm, close to estimated laser threshold.

The laser structures were grown by solid source MBE in Riber Compact 21T reactor. The beams of the group III elements (6.5N Al and 7N Ga) were generated by using the standard ABN 80 DF effusion cells. The beam of  $As_4$  molecules was produced by the valved-cracker As effusion cell. The (100) oriented GaAs n+ substrates supplied by AXT, Inc. were used. The substrate temperature  $T_s$ , controlled on the surface of the growing crystal by a pyrometer, was kept at 580 °C. The value of V/III ratio was at least 35 for growth of both GaAs and  $Al_{0.45}Ga_{0.55}As$  layers.

The GaAs growth rate  $V_{GaAs}$  was adjusted by reflection high energy electron diffraction (RHEED) intensity oscillations as equal to 0.5 ML/s. The corresponding gallium flux was kept constant during the growth of the whole QCL structure. The growth rate  $V_{AlAs}$  of AlAs was adjusted to match the 45% of this binary in AlGaAs barriers, and was subsequently confirmed by high-resolution X-ray diffractometry (HRXRD) on test superlattices. The corresponding aluminum flux was then applied during the growth of the whole QCL structure. No growth interruptions between the individual layers within the active region were applied. Hence, only the Al effusion cell was activated and closed during the QCL growth run, according to the need.

The principle of operation of QCL structures places stringent requirements on the individual layer thickness and composition as well as the overall periodicity of the whole structure. The laser operation is possible only when the designed structure is strictly realized, with the extreme technological precision concerning geometrical and doping features. That is why the technology of epitaxy used for QCLs must be characterized by perfect long time stability of growth parameters as well as run-to-run reproducibility. For the development of QCL structures, besides the laser structures, a large number of different superlattice test structures were grown and characterized. Detailed analysis of the growth optimization procedures can be found in ref. [3].

To obtain information about the thickness and composition of component layers of both test structures and complete QCL structures, a theoretical analysis of double-crystal rocking curves was carried out. The dynamical diffraction theory has been used for simulating the symmetric (004) reflections, leading to the extraction of structural parameters of periodic structures. Detailed analysis of measured HRXRD triple-axis  $2\theta/\omega$  scans (see Fig.3) documents almost perfect agreement between optimized laser structure and simulated one referring to the intended design. This is seen from matching the measured and calculated satellite peak positions. Better than 1% thickness accuracy has been routinely achieved

for lasing structures. The barrier layers have been found to contain  $(45 \pm 1)\%$ , which is, however, not that critical for lasing as thickness inaccuracy. The on-line HRXRD measurements have been found crucial for QCL technology development.

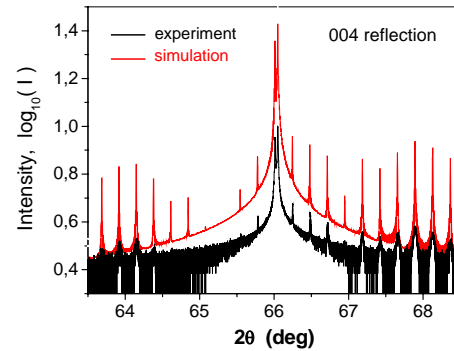


Fig. 3 Comparison of the experimental and simulated HRXRD  $2\theta/\omega$  scans for QCL structure. The simulated curve has been shifted upwards for clarity.

All the above mentioned features document strict periodicity of the structures, which has been additionally confirmed by TEM results (see Fig.4). However, the precision of thickness determination from TEM was lower than the one obtained from HRXRD measurements.

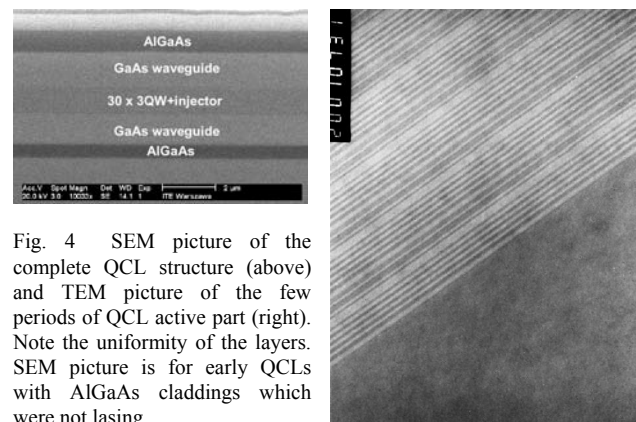


Fig. 4 SEM picture of the complete QCL structure (above) and TEM picture of the few periods of QCL active part (right). Note the uniformity of the layers. SEM picture is for early QCLs with AlGaAs claddings which were not lasing.

The double trench lasers were fabricated using standard processing technology, i.e., wet etching and  $Si_3N_4$  for electrical insulation. The low resistivity Ni/AuGe/Ni/Au ohmic contacts, alloyed in 430 °C, were used at the top of the devices. For current injection, windows were opened through the insulator with width 25, 35, and 50  $\mu m$ . After the wafer was thinned down to about 100  $\mu m$ , an alloyed AuGe/Ni/Au contact was deposited on the backside. The lasers were cleaved into bars of 0.5, 1 and 2 mm length and soldered with Au/Sn eutectic, epilayer down on diamond heatspreader and copper submounts. The basic electrical characterization was carried in the temperature range from 77 K to 300 K.

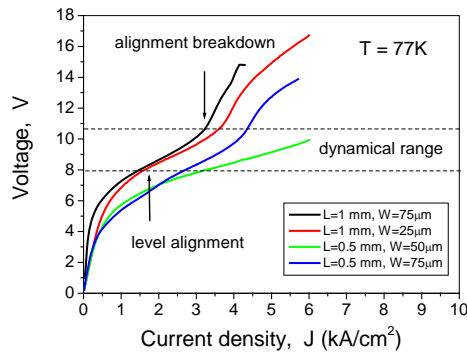


Fig. 5 Voltage versus current characteristics for  $\text{Al}_{0.45}\text{Ga}_{0.55}\text{As}/\text{GaAs}$  QCLs with low injector doping ( $4 \times 10^{11} \text{cm}^{-2}$  per period). The devices were driven 2  $\mu\text{s}$  pulses with repetition rate of 0,5 kHz.

Figure 5 shows V-I characteristics for lasers with different resonator length  $L$  and ridge width  $W$ . At low bias QCL structures are highly resistive. After the electric field has reached value  $\approx 40 \text{ kV/cm}$  (voltage drop  $\approx 8 \text{ V}$ ) electrons start flowing through the device. In this regime the operating voltage increases linearly with injection current. The saturation of the V-I characteristics, observed at about 11 V, is caused by the onset of misalignment between the upper laser level and the injector ground state. This effect depends on the injector doping density and limits the dynamic range of laser operation [4],[5]. The linear part of the V-I characteristics can be fitted with equation:  $V(I) = V_{\text{to}} + R_d I$ , with the turn on voltage  $V_{\text{to}} = 8 \text{ V}$  and differential resistance  $R_d$ , which varied from  $0.75 \Omega$  to  $1.5 \Omega$  for the investigated devices. To achieve lasing the injector doping had to be increased substantially to allow for higher currents before the saturation.

Light output and current-voltage characteristics of the laser fabricated from  $\text{GaAs}/\text{Al}_{0.45}\text{Ga}_{0.55}\text{As}$  heterostructure with injector doping  $\approx 2.2 \times 10^{12} \text{cm}^{-2}$  are shown in Fig. 6.

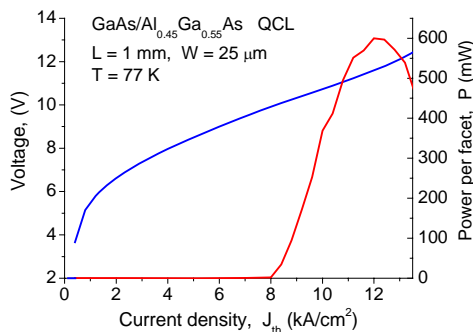


Fig. 6 77 K light – current and current - voltage characteristics of the  $\text{GaAs}/\text{Al}_{0.45}\text{Ga}_{0.55}\text{As}$  laser driven by 2  $\mu\text{s}$  pulses with repetition rate of 0.5 kHz. The laser emission was recorded with TE cooled HgCdTe detector (type PVI-2TE-10- Vigo System S.A.). Light from the laser was shined directly on the detector (no collimating lens was used). The detector active area was  $0.3 \times 0.3 \text{mm}^2$ .

The threshold current density can be calculated from the equation [6]:

$$J_{th} = \frac{\epsilon_0 n \lambda L_p \gamma_{32}}{4 \pi e \Gamma |z_{32}|^2} \frac{\alpha_w + \alpha_m}{\tau_3 (1 - \tau_{21} / \tau_{32})} \quad (1)$$

where an injection efficiency of unity in the upper laser level E3 is assumed and direct tunneling processes out of levels E2 and E3 are neglected. In this equation,  $\epsilon_0$  is the vacuum permittivity,  $n$  is effective refractive index of the laser mode,  $\lambda$  is the emission wavelength,  $L_p$  is the length of one segment,  $\gamma_{32}$  is the full width at the half maximum (FWHM) of the spontaneous emission spectrum,  $e$  is electron charge,  $\Gamma$  is the confinement factor and  $z_{32}$  is the matrix element of the laser transition. The scattering times  $\tau_{ij}$  from states  $i$  to  $j$  are dominated by LO-phonon emission [6]. The mirror losses  $\alpha_m = -\ln(R_1 R_2)/2L$  depend on cavity length and mirror reflectivities. For uncoated mirrors  $R_1 = R_2 \approx 0.29$ . The waveguide losses  $\alpha_w$  are estimated to be equal to  $25 \text{ cm}^{-1}$ , the confinement factor  $\Gamma = 0.27$  and the effective refractive index  $n$  is 3.27[7]. For the investigated design  $\lambda = 8.4 \mu\text{m}$ ,  $\tau_{32} = 2.1 \text{ ps}$  and  $\gamma_{32} = 16 \text{ meV}$ . Inserting the values given above into Eq.(1) we get  $J_{th}$  for the 1 mm long device equal to  $\approx 6.7 \text{ kA/cm}^2$ , which is in full agreement with the experimental result.

We report the design and fabrication of GaAs based QCLs emitting at  $9 \mu\text{m}$ . The devices operated at 77 K, in pulsed mode with powers up to 600 mW and slope efficiency  $\eta \approx 0.72 \text{ W/A}$  per uncoated facet.

The authors would like to acknowledge L. Ornoch, and J. Kaniewski for help in the electrical measurements, I. Sankowska for XRD measurements and J. Piotrowski (Vigo System S.A.) for providing thermoelectrically cooled HgCdTe detector. The continuous support of A. Gago is also greatly acknowledged. The work was financially supported by Grant PBZ-MIN-02/I/2007.

## References

- [1] H. Page, C. Becker, A. Robertson, G. Glastre, V. Ortiz, C. Sirtori, Applied Physics Letters, vol.78., 3529 (2001).
- [2] P. Harrison, Quantum Wells, Wires and Dots: Theoretical and Computational Physics, 2<sup>nd</sup> ed., Chichester, U.K.: Wiley 2005
- [3] K. Kosiel, J. Kubacka-Traczyk, P. Karbownik, A. Szerling, J. Muszalski, M. Bugajski, P. Romanowski, J. Gaca, M. Wójcik, Microelectronics Journal, (2008), in print
- [4] S. Hofling, V. D. Jovanovic, D. Indjin, J. P. Reithmaier, A. Forchel, Z. Ikonc, N. Vukmirovic, P. Harrison, Appl. Phys. Lett., vol. 88, 251109 (2006)
- [5] Ch. Mann, Q. Yang, F. Fuchs, W. Bronner, K. Kohler, J. Wagner, IEEE J. Quantum Electronics, vol. 42, 994 (2006)
- [6] H. C. Liu, F. Capasso, *Intersubband transitions in quantum wells – physics and device applications II*, Semiconductors and Semimetals, vol. 66, Academic Press, New York 2000
- [7] S. Hofling, R. Kallweit, J. Seufert, J. Koeth, J. P. Reithmaier, A. Forchel, J. Crystal Growth, vol. 278, 775 (2005)